# *A supramolecular glass made from a low molecular weight amino acid derivative*

# A supramolecular glass made from a low molecular weight amino acid derivative

B.C. Baker,[a*†] A.D. O'Donnell,[a] Priya,[a] M. Hyder,[a] I.M. German,[b] and W. Hayes[a*]

[a]*Department of Chemistry, University of Reading, Whiteknights, Reading, RG6 6DX, U.K.*

[b]*Kinectrics Inc., 17-18 Frederick Sanger Road, The Surrey Research Park, Guildford, Surrey, GU2 7YD, U.K.*

*Email: w.c.hayes@reading.ac.uk.*

[†] *Present address: Department of Chemistry, University of Bristol, Cantock's Close, Bristol, BS8 1TS, U.K.*

**Abstract:** A low molecular weight tyrosine derivative with self-assembling capabilities has been found to form a robust optically transparent supramolecular glass after casting at 70 °C. The glass films are remarkably stable, remaining transparent over 12+ months as well as in contact with water and can be reprocessed via solvation in a wide range of organic solvents. The solubility, long-term stability and thermo-responsive properties of the bio-derived glass makes it an ideal candidate for use as a window where its reprocessability at easily accessible temperatures are attractive.

**Keywords:** Supramolecular; self-assembly; transparent glass; amino acid; reprocessability

**Introduction**

Amorphous glassy materials are observed frequently in polymer structures, but structures that are far lower in molecular weight (<1000 g/mol, termed 'molecular glasses' [1]) have also recently been found to possess the ability to form amorphous and transparent materials with ambient glass transition temperatures ($T_g$ > 25 °C). The advantages of working with lower molecular weight materials over polymeric counterparts are their well-defined molecular structure, increased purity, processability and tunability of properties via simple structural modifications.[2] One key beneficial property is the increased solubility of molecular glasses in organic solvents presenting a route to reprocessing for the optically transparent materials at ambient or easily accessible temperatures in the event of damage.[3]

Low molecular weight materials tend to reach thermodynamic equilibrium quickly, thereby converting amorphous forms into ordered crystalline phases.[2,4,5] Few low molecular weight glasses can forestall this process indefinitely, especially at temperatures above their glass transition temperature, $T_g$. Studies of the self-assembly processes of low molecular glasses are yet to be described in great detail.[1-7] Furthermore, self-supporting, standalone molecular glasses that are not reliant upon film or alternative supportive media for stability or blending plasticizers to achieve desired transparency, tensile and rheological properties are rare.[1-8]

In this paper we report the synthesis of an optically transparent molecular glass derived from the naturally occurring amino acid tyrosine. Whilst elegant examples of amino acid based functional polymers have been reported, [9-10] discrete low molecular weight amino acid-derived materials capable of forming stable films have not been described. In this study tyrosine was selected as an abundant amino acid, with π-π stacking capabilities as well as use in polymeric glasses [11]. Furthermore, the observed difference in the melt characteristics of tyrosine upon esterification, when

combined with our knowledge of the urea self-assembly group in low molecular weight gelators [12] made tyrosine an ideal starting material for this fundamental materials study. The glass not only functions as an optically transparent film on supporting materials but a method involving thermal casting onto a polymeric support, and subsequent removal, delivers a standalone/self-supporting optically transparent film. The self-assembly of this tyrosine derivative was probed by VTIR and NMR spectroscopies to characterise the amorphous phase associations.

**Experimental**

**Materials and Methods**

All of the chemicals and solvents were purchased from Sigma Aldrich and used as purchased. THF was distilled from sodium and benzophenone under inert conditions prior to use. All other solvents were used as supplied. NMR spectra were obtained using Bruker Nanobay 400 and Bruker DPX 400 (operating at 400 MHz and 100 MHz for $^{1}$H NMR and $^{13}$C NMR, respectively). All samples were prepared in either acetonitrile-$d_3$ or DMSO-$d_6$ and dissolution was achieved with slight heating and sonication (5-10 minutes). A Perkin Elmer 100 FT-IR (diamond ATR sampling attachment) was employed for IR spectroscopic analysis. All the samples in the characterisation were cast from THF in solid form. Mass spectra were generated from Thermo-Fisher Scientific Orbitrap XL LCMS (operating in electrospray mode)—samples were prepared in either 0.1 M NaOH(aq) or DMSO (for direct injection) (1 mg mL$^{-1}$). Thermogravimetric Analysis employed a TA Instruments TGA Q50 system attached to TGA heat exchanger, platinum crucible and an aluminium TA-Tzero pan (ramp rate 10 °C/min to 400 °C). Differential scanning calorimetry analysis employed a TA DSC Q2000 with TA Refrigerated Cooling System 90 (aluminium TA-Tzero pans and lids) (ramp rate 10 ˚C/min). Rheological analysis employed TA Instruments AR 2000 rheometer operating in the plate geometry (20 mm steel plate, with a frequency sweep of 0.2-16 Hz, G' and G" selected at the maximum shear modulus of each temperature sweep). UV spectra were recorded using a Varian Cary 300 Bio or a PerkinElmer Lambda 25 UV/Vis Spectrometer. Samples were analysed in quartz cuvettes with a 5.0 mm path length and were baseline corrected with respect to a blank cell with the appropriate solvent. The solid-state UV/Vis-NIR spectra were recorded on a Shimadzu UV-2600 Spectrometer. Specific optical rotation was monitored via a Bellingham + Stanley Ltd Polarimeter ADP610 with a 589 nm Wavelength and Peltier temperature control apparatus as 22 °C at 7.0 mg/mL in a 20mm path length.

To form casts of **1L** on glass, approximately 0.1g of **1L** was placed on a flat silica glass slide support (26 × 76 × 1 mm) and heated to 70 °C for 10 minutes. To form stand-alone casts, approximately 0.2 g of **1L** was placed between two casts of the silicone rubber ecoflex® (each ecoflex cast weighed *ca*. 1.0 g) and the assembly was held at 70 °C for 30 minutes with compression achieved via application of a 2.0 g weight on the top of the casts – this was allowed to cool to room temperatures (*ca*. 25 °C) before the ecoflex® casts were removed. Disks of KBr and **1L** were prepared by mixing at room temperature and then cast under 10 tons of pressure. The IR spectra of the disks were recorded in the 400 − 4000 cm$^{-1}$ wavenumber region using a using a Perkin Elmer 100 FT-IR (Fourier Transform Infrared) instrument equipped with a Specac variable temperature transmission cell holder. Each spectrum was the accumulation of 32 scans at 4 cm$^{-1}$ resolution. The spectrum of the unblended KBr disk was initially recorded as the background at all temperatures. Transmission spectra of **1L** disk was recorded and analysed from 25 to 65 °C, with their spectra being recorded at ∼5 °C intervals; each temperature step allowed to equilibrate for 5 minutes before the spectra were recorded. Temperatures below 25 °C were found to accumulate too much water vapour from the atmosphere to allow meaningful results to be calculated. Temperatures were controlled using the Specac variable temperature cell controller system. The temperature was measured locally with a thermocouple embedded inside the solid cell frame. For each temperature, the difference of absorbance A(**1L** KBr) − A(KBr) was plotted. Data were

analysed under the OriginLab software, and the absorbance data was deconvoluted into a sum of single Gaussian signals using the "spectral fit" module (see the supporting information (SI), **Figure S1** and **Table S1**).

**Synthesis and characterisation data**

**L-tyr-methyl** or **D-tyr-methyl** was reacted with a molar equivalent of 4-nitrophenyl isocyanate in the presence of triethylamine (5 mL) at room temperatures (25 °C) in THF (30 mL) to give the desired tyrosine urea derivative, isolated by filtration (45 μm) then removal of the solvent *in vacuo,* to yield;

**1L** as a yellow powder (198 mg, 84 % yield); $^{1}$H NMR (400 MHz, $CD_3CN$-$d_3$) δ 8.10 (AA'XX', 2H), 7.87 (s, 1H), 7.55 (AA'XX', 2H), 7.03 (AA'XX', 2H), 6.87 (s, 1H), 6.74 (AA'XX', 2H), 5.63 (d, $J$ = 7.8 Hz, 1H), 4.62 (X of ABX, $J_{AX}$ = 6.18 Hz, $J_{BX}$ = 6.19 Hz, 1H), 2.99 and 3.02 (AB of $A_{BX}$, $J_{AB}$ = 14.03 Hz, $J_{AX}$ = 6.18 Hz, $J_{BX}$ = 6.19 Hz, 2H) ppm.$^{13}$C{H} NMR (100 MHz, $CD_3CN$-$d_3$) δ 173.4, 156.9, 154.8, 147.1, 142.8, 131.5, 128.5, 125.9, 118.3, 116.2, 55.2, 52.8, 37.6 ppm. IR (ATR)/cm$^{-1}$ 3348, 2982, 1728, 1677, 1612, 1598, 1554, 1504, 1441, 1329, 1301, 1209, 1173, 1109, 836, 749, 689, 530. $[\alpha]^{D}_{22}$ = -12.2 (c, 7.0 mg/10 mL in EtOH). $T_{deg}$ (5 % wt. loss 165.6 °C, 10 % wt. loss 201.4 °C). $T_g$ (26.3 °C). MS (ESI) m/z [M+H$^+$] calculated for $C_{17}H_{18}N_3O_6$ = 360.1190, found = 360.1189.

**1D** as a yellow powder (156 mg, 73 % yield); $^{1}$H NMR (400 MHz, $CD_3CN$-$d_3$) δ 8.13 (AA'XX', 2H), 7.90 (s, 1H), 7.58 (AA'XX', 2H), 7.03 (AA'XX', 2H), 6.90 (s, 1H), 6.77 (AA'XX', 2H), 5.64 (d, $J$ = 8.0 Hz, 1H), 4.62 (X of ABX, $J_{AX}$ = 6.16 Hz, $J_{BX}$ = 6.20 Hz, 1H), 2.99 and 3.02 (AB of $A_{BX}$, $J_{AB}$ = 14.03 Hz, $J_{AX}$ = 6.16 Hz, $J_{BX}$ = 6.20 Hz, 2H) ppm. $^{13}$C{H} NMR (100 MHz, $CD_3CN$-$d_3$) δ 172.6, 156.1, 154.1, 146.2, 141.9, 130.6, 127.5, 125.0, 117.5, 117.4, 115.3, 54.4, 51.9, 36.7. IR (ATR)/cm$^{-1}$ 3360, 2956, 1727, 1677, 1614, 1598, 1553, 1505, 1441, 1329, 1304, 1214, 1176, 1112, 850, 750, 691, 530. $[\alpha]^{D}_{22}$ = +9.4 (c, 7.0 mg/10 mL in EtOH). $T_{deg}$ (5 % wt. loss 162.4 °C, 10 % wt. loss 197.5 °C). $T_g$ (25.8 °C). MS (ESI) m/z [M+H$^+$] calculated for $C_{17}H_{18}N_3O_6$ = 360.1190, found = 360.1193.

**Results and Discussion**

***Synthesis and Characterisation*** The tyrosine derivative capable of forming a bio-based amorphous glass (**1L**) was accessed via initial protection of the amino acid, L-tyrosine (**L-tyr**) to form the methyl ester hydrochloride salt (**L-tyr-methyl**), from a modification of a reaction procedure previously reported by Vimal *et al*.[13,14] **L-tyr-methyl** was then reacted with a molar equivalent of 4-nitrophenyl isocyanate in the presence of triethylamine and filtered to remove the insoluble ammonium hydrochloride salt. The desired tyrosine urea derivative **1L** was isolated by removing the solvent *in vacuo* to yield an amorphous yellow powder (**Scheme 1**). The synthesis of **1L** was confirmed via $^{1}$H NMR spectroscopic analysis. Resonances were evident at 6.87 and 5.83 ppm, respectively, correlating to the urea protons (thus confirming formation of urea linkages rather than urethanes) and two sets of AA'XX' resonances were observed (8.10, 7.55, 7.03 and 6.74 ppm) corresponding to the two 1,4-disubstituted aromatic units (see supporting information, **Figure S2**). $^{13}$C{H} NMR, infrared and mass spectroscopic analysis (**Figures S3-5**) also revealed the presence of the ester and urea carbonyl resonances and absorbances at 173.4/156.9 ppm and 1793/1614 cm$^{-1}$, respectively, in **1L**. The enantiomer **1D** was also synthesised successfully from D-tyrosine (for characterisation data see **Figure S6-9**), using the same procedure.

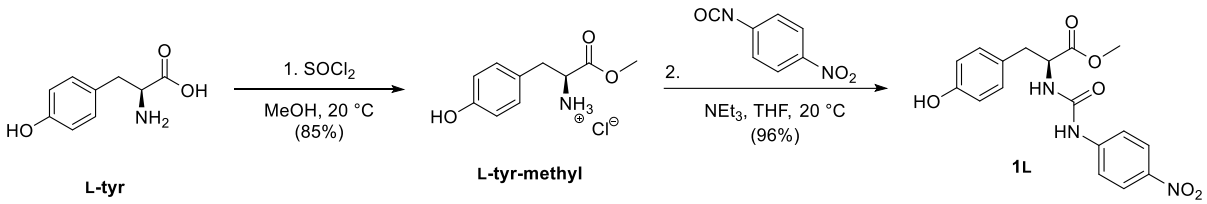


**Scheme 1** Synthetic procedure for the formation of the tyrosine urea derivative **1L** from the amino acid **L-Tyr**

***Glass formation studies*** To form the amorphous glass casts the yellow powder of **1L** was heated at 70 °C for 10 minutes on a flat silica glass slide support to produce optically transparent yellow coatings (*ca*. 0.5 mm thick, with a variety of coloured backgrounds being observed through the coating, see **Figure S10**). Although a melt was observed by eye (at 68 – 72 °C), no observable melt transitions were recorded by differential scanning calorimetry (DSC) analysis. Furthermore, at temperatures higher than 90 °C it was found that the material did not flow sufficiently for useful casts to be made, though transparency was maintained. Casts of **1L** were also formed via compression moulding at 70 °C between the casted silicone rubber ecoflex® to give transparent self-supporting optically transparent film (**Figure 1a**). Confirmation of the structural integrity of the small molecule after casting was obtained by $^{1}$H NMR spectroscopic analysis (identical spectra were observed for the compound before and after casting, see **Figures S11** and **S12**) as well as a lack of exotherms (associated with chemical reactions) in the primary DSC heat cycles indicating the reprocessability of the transparent slides. Indeed, several experiments to demonstrate the reprocessability were undertaken in the form of solvent dissolution of casts in acetone, solvent removal and recasting (see **Figure S13**), as well as recasting of broken films via thermal press (again moulding at 70 °C, **Figure S14**).

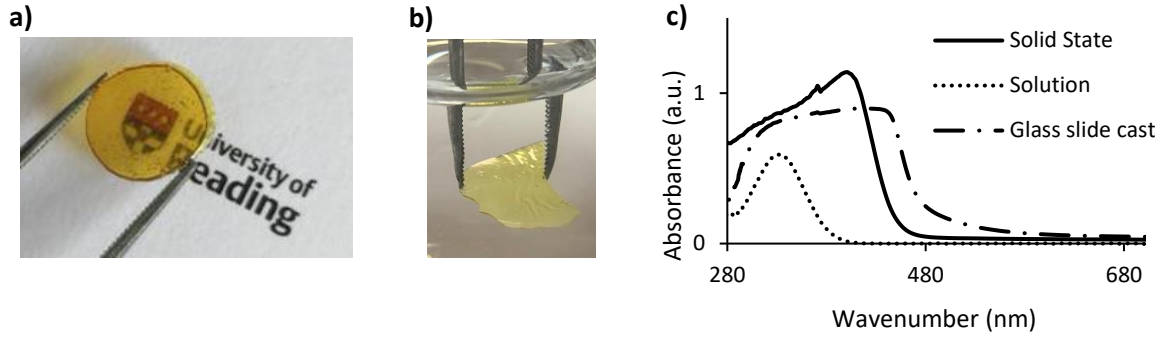


**Figure 1 a)** Compression moulded (under 25 Pa) slide of **1L** (*ca*. 1.5 mm thickness) demonstrating the optical transparency of the formed plate, b) melt cast fragment of **1L** in water, **c)** UV-vis spectroscopic data of **1L** films in the solid state and cast on glass substrate (*ca*. 0.5 mm thickness) (source of UV-radiation change at 323 nm) and solution state (acetonitrile).

Interestingly it was found that transmittance of several coloured backgrounds was obtainable through the cast objects (**Figure S10**) demonstrating transmittance of the film in the visible wavenumber region. Furthermore, exposing the cast tyrosine urea derivative **1L** to water did not result in dissolution or loss of transparency (**Figure 1b**). The casts were, however, soluble in a range of organic solvents including, methanol, ethanol, THF, DMSO and acetonitrile, which enabled reusability *via* recasting from dissolution then solvent removal. Once formed, the casts were found to retain transparency (i.e. not crystallise) for long periods from monitoring for 12+ months. The UV-vis absorbance characteristics of **1L** were explored using acetonitrile solutions, and in the solid thin film state cast on quartz plates as well as cast on glass support slides. The absorption spectra recorded in the solution phase revealed the vibronic structure associated with many self-assembling nitro-aromatics

(absorbance maximum around 335 nm, **Figure 1c**).[12] In the UV-visible spectrum of **1L** in the solid state, the $\lambda_{max}$ absorbance was red-shifted (405 nm) when compared to the solution state form (335 nm). However, the absorption range of both samples was located predominantly in the purple to deep-blue region affording **1L** a visible yellow colour – the red shift for the solid state sample was attributed to an increase in the order of the system upon solvent removal.[15,16]

To monitor the effect of enantiomeric excess on the transparency of the glass, a cast of a 1:1 mixture of the enantiomer **1D** with **1L** on a silica glass support was compared with enantiopure casts of **1D** and **1L**. Transparency was achieved in each sample (**Figure S10**). It was noted that neither the unprotected **L-tyr** or methylated **L-tyr-methyl** starting materials (both in salt and free amine form) produced transparent or stable films under the same casting conditions, forming powder like, or charred materials, respectively (**Figure S10**).[13-14]

***Solid state assembly studies*** To understand the nature of self-assembly of **1L** several solid-state analytical experiments were undertaken. Variable temperature infra-red spectra were recorded from 25 – 65 °C to monitor the relative absorbances from bound and unbound carbonyl groups. The samples were prepared as KBr discs with a loading of **1L** of 0.1 % wt. This approach ensured homogeneity throughout the beam path at all temperatures, samples cast directly onto KBr discs or glass slides were found to afford variable absorbance changes because of material flow at the higher temperatures studied. Analysis of the spectra of **L-tyr**, **L-tyr-methyl** and **1L** both in solid state and in acetonitrile revealed the absorbances associated with hydrogen bonded and free carbonyl stretch of the urea (1680 and 1703 $cm^{-1}$, respectively) and ester (1725 and 1745 $cm^{-1}$, respectively) moieties (**Figure S15**). [17-20]. With these assigned absorbances heating of the KBr discs with a loading of **1L** revealed distinct variations in the absorbances associated with hydrogen bonded and free carbonyl stretches of the urea and ester (1675 and 1739 $cm^{-1}$, respectively) (see **Figure S16**). Deconvolution of these absorbances enabled the percentage integrals of both bound and unbound carbonyl ester and urea stretch frequencies as a function of temperature to be determined (**Figure 2**, see **Figure S1** and **Table S1** for deconvoluted examples and parameters). Comparison of the normalised integrals of the absorbances assigned to the bound and unbound ester and urea carbonyls throughout the heating cycle revealed three thermal regions of interest. Firstly, a shift was observed towards greater proportions of free ester and urea when heating from 25 to 60 °C (region *i*, **Figure 2**). The glass transition ($T_g$) for **1L** was recorded by DSC at 26 °C (**Figure S17**) indicating that the transition is likely caused by a move from hydrogen bound to unbound systems but that the overall dominance of the bound urea gives physical stability to the system.[21] Secondly, as the temperature was elevated above 65 °C towards the casting temperature (70 °C), an unexpected dissociation of the ureas along with an increase in bound esters (region *ii*, **Figure 2**) implies structural reordering within the bulk phase (although the process does not facilitate crystallisation).[2,5] As the system was held above 90 °C the free urea and esters maintain a plateau (region *iii*, **Figure 2)**. Interestingly, limited change was observed in the heating/cooling of **1L** when observing the NH/OH region (see **Figure S16**).

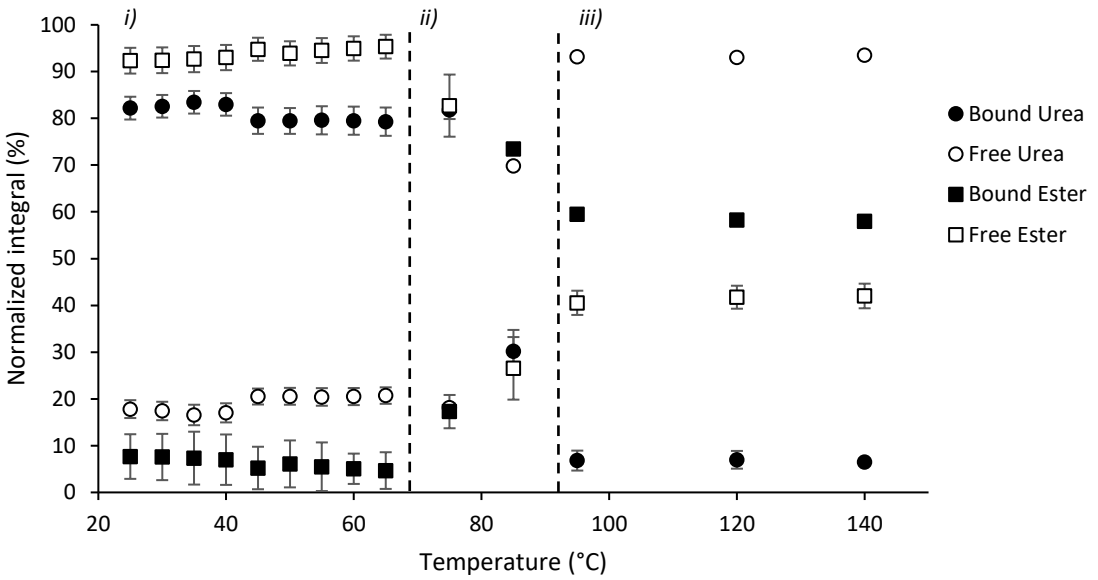


**Figure 2,** Normalised integrals (after deconvolution into a sum of single Gaussian signals) of heated IR sample of **1L** (loaded in a KBr disc, with KBr:**1L** 1:0.1 % wt) recorded across the temperature range: 25-140 °C after deconvolution of absorbances assigned to free and bound ester and urea carbonyls in samples of **1L,** utilising **Figure S1**, error bars shown as a percentage from a Gaussian fit after deconvolution, where *i)-iii)* refer to regions for reference throughout the text.

***Solvated assembly studies*** To further probe the self-assembly properties of **1L** $^{1}$H NMR titration studies in deuterated acetonitrile were conducted. It was observed that hydrogen bonding interactions associated with the urea and phenolic motifs were dominant, the influence of π-π stacking being negligible (for a more detailed discussion see SI and **Figures S18**-**19**). The limited influence of π-π stacking within the system was further corroborated by the fact that the $\lambda_{max}$ absorbance showed little dependence on aprotic or protic solvents (338 and 335 nm in acetonitrile and ethanol solution, respectively, see the dotted line in **Figure 1c** and **Figure S20**).

Interestingly attempts to gel **1L** in either organic or aqueous media proved unsuccessful, a surprising result when compared to the excellent gelling abilities of analogous (but achiral) bis aromatic nitro urea compounds [12] and amino acid systems reported independently by the Adams,[22] Smith[23] and Ulijn[24] groups.

***Thermal Analysis*** To assess the thermal stability of **1L** and **1D** several experiments were undertaken. Thermogravimetric analysis (TGA) was undertaken on both samples (under inert conditions, heating rate of 10 °C/min to 600 °C) revealing stability up to 160 °C at 5 %wt loss and 199 °C 10 %wt loss for both compounds (**Figure S21**) attributed to absorbed atmospheric water (with ester and urea bond degradation proceeding at > 200 and > 300 °C, respectively).[25] No significant weight loss (< 1% wt) was recorded in the casting temperature region 65 – 100 °C. Differential scanning calorimetric analysis of blends of **1L** and **1D** (as well as in isolation) revealed limited variation on the materials $T_g$ values (**Figures S17, S22-24**) indicating a lack of a 'majority-rule-like-effect'.[26,27]

Rheological analysis of **1L** was undertaken to assess the thermo-responsiveness of the materials (**Figure 3**). Frequency sweeps were performed to measure the viscoelastic properties at a fixed shear strain of 0.5% at varying temperatures (**Figure 3a**). At temperatures below 65 °C and above 100 °C the material proved too stiff to achieve meaningful results. At temperatures above 65 °C the material responded as a viscoelastic liquid with loss modulus (G'') exceeding the storage modulus (G'). Most interestingly an inversion of G' and G'' was observed between temperatures of 75 to 85 °C, with the

compound moving from a highly viscous liquid to a semi solid between these temperatures (**Figure 3b**). These results were further corroborated by analysis of the individual frequency sweeps of **1L** at different temperatures. At 65 °C the molecular glass behaves as a viscoelastic liquid, with the loss modulus being an order of magnitude higher than that of the storage at low frequencies (long time scale). On shorter time scales (high frequencies) G" becomes less dominant, a behaviour that is typically seen in glass-like materials.[28] Interestingly, at 95 °C the material behaves as a glass, where G' exceeds G''.

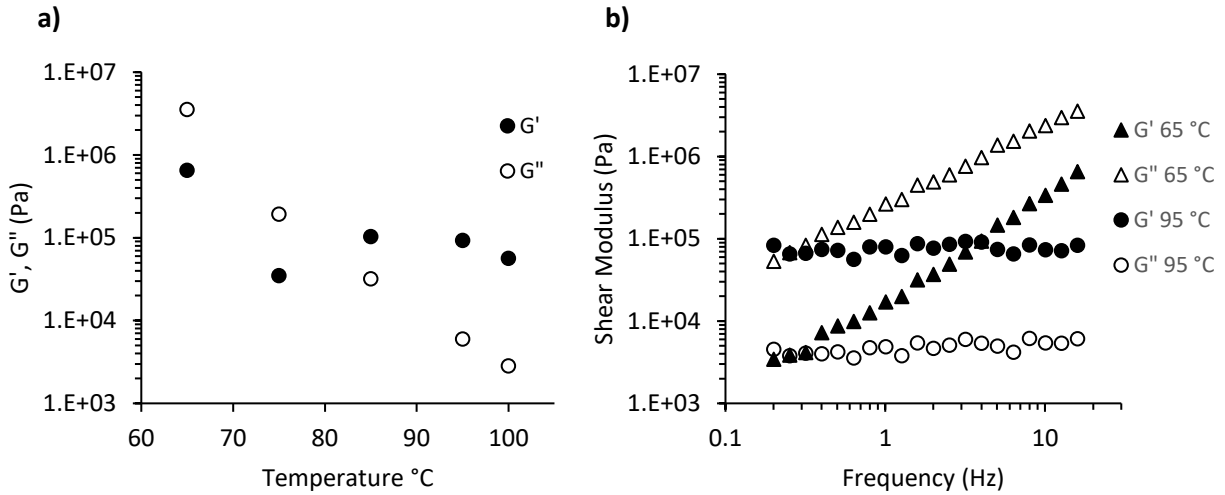


**Figure 3. a**) maximum storage (G') and loss (G") modulus a function of temperature of **1L**, **b)** G' and G" modulus of **1L** frequency sweeps for temperatures 65 °C and 95 °C (parallel plate-plate geometry, shear strain 0.5 %).

## Conclusions

In summary, we have synthesised an amino acid based supramolecular material which is capable of self-assembling upon thermosetting to produce a transparent self-supporting glass. The optical properties of this material are not reliant upon the enantiomer present, so the glasses may be derived from the naturally occurring amino acid. The self-assembly behaviour of this amino acid urea derivative relies upon a balance of hydrogen bonding between the urea and ester moieties of the molecule throughout the casting temperature range. The biological availability of the starting materials, low processing temperatures to form the glasses and the potential for reusability of the cast glasses of the molecule make this a highly promising system.

## Supporting Information

The Supporting Information is available free of charge:

Characterization data (NMR, IR, VT-IR, UV, MS, DSC, TGA, Rheology)

## AUTHOR INFORMATION

### Corresponding Author

* w.c.hayes@reading.ac.uk

### Author Contributions

The manuscript was written through contributions of all the authors.

### Acknowledgments

The authors would like to acknowledge financial support from the University of Reading and Kinectrics UK Ltd (PhD studentships for B.C.B. and A.O'D.) and the Ministry of Social Justice and Empowerment (Government of India) for Priya. In addition, the University of Reading is acknowledged for granting access to instrumentation in the Chemical Analysis Facility.

**References**

[1] D. K. Hohl, A.C. Ferahian, L. Montero de Espinosa, C. Weder, Toughening of Glassy Supramolecular Polymer Networks, ACS Macro Lett. 8 (2019) 1484-1490. https://doi.org/10.1021/acsmacrolett.9b00710.

[2] L. Yu, Surface mobility of molecular glasses and its importance in physical stability, Adv. Drug Del. Rev. 100 (2016) 3-9. https://DOI: 10.1016/j.addr.2016.01.005.

[3] R. Vadrucci, C. Weder, Y.C. Simon, Low-power photon upconversion in organic glasses, J. Mater. Chem. C 2 (2014) 2837-2841. https://doi.org/10.1039/C3TC32473G.

[4] C. Bhugra, M.J. Pikal, Role of thermodynamic, molecular, and kinetic factors in crystallization from the amorphous state, J. Pharm. Sci. 97 (2008) 1329–1349. https://doi.org/10.1002/jps.21138.

[5] Y. Sun, L. Zhu, T.Wu, T. Cai, E.M. Gunn, L. Yu, Stability of Amorphous Pharmaceutical Solids: Crystal Growth Mechanisms and Effect of Polymer Additives, AAPS J. 14 (2012) 380-388. https://doi.org/10.1208/s12248-012-9345-6.

[6] A. Laventure, D. Lauzon, C. Pellerin, O. Lebel, Triazine-based molecular glasses frustrate the crystallization of barbiturates, Cryst. Eng. Comm. 21 (2019) 1734–1741. https://doi.org/10.1039/C9CE00022D.

[7] S. Boileau, L. Bouteiller, E. Foucat, N. Lacoudre, Stable low molecular weight glasses based on mixtures of bisphenol-A and bispyridines, J. Mater. Chem., 12 (2002) 195-199. https://doi.org/10.1039/B106234B

[8] D.W.R. Balkenende, C.A. Monnier, G.L. Fiore, C. Weder, Optically responsive supramolecular polymer glasses, Nat. Commun. 7 (2016) 10995. https://doi: 10.1038/ncomms10995 (2016).

[9] C. L. Zaccaria, V. Cedrati, A. Nitti, Enrica Chiesa, A. Martinez de Ilarduya, M. Garcia-Alvarez, M. Meli, G. Colombo and D. Pasini, Biocompatible graft copolymers from bacterial poly(γ-glutamic acid) and poly(lactic acid), Polym. Chem. 12 (2021), 3784-3793. https://doi.org/10.1039/D1PY00737H

[10] V. Cedrati, A.Pacini, A. Nitti, A. Martínez de Ilarduya, S. Muñoz-Guerra, A. Sanyal and D. Pasini, "Clickable" bacterial poly(γ-glutamic acid), Polym. Chem. 11 (2020), 5582-5589. https://doi.org/10.1039/D0PY00843E

[11] V. Tangpasuthadol, A. S. Kimberly, A. Hooper, J. Kohn , Thermal properties and physical ageing behaviour of tyrosine-derived polycarbonates, Biomaterials, 17 (1996) 463-468. https://doi.org/10.1016/0142-9612(96)89665-7

[12] a) F. Rodgriguez-Llansola, B. Escuder, J.F. Miravet, D. Hermida-Merino, I.W. Hamley, C.J. Cardin, W. Hayes, Selective and highly efficient dye scavenging by a pH-responsive molecular hydrogelator, Chem. Commun. 46 (2010) 7960-7962. https://doi.org/10.1039/C0CC02338H; b) D.M. Wood, B.W. Greenland, A.L. Acton, F. Rodríguez-Llansola, C.A. Murray, C.J. Cardin, J.F. Miravet, B. Escuder, I.W. Hamley, W. Hayes, pH-Tunable Hydrogelators for Water Purification: Structural Optimisation and Evaluation, Chem. Eur. J. 18 (2012) 2692–2699. https://doi.org/10.1002/chem.201102137; c) B.C. Baker, A.L. Acton, G.C. Stevens, W. Hayes, Bis amide-aromatic-ureas—highly effective hydro- and

organogelator systems, Tetrahedron 70 (2014) 8303-8311. https://doi.org/10.1016/j.tet.2014.09.017

[13] C.A. Faler, B. Cao, M.M. Joullié, Synthesis of Bicyclic Cyclopropylamines from Amino Acid Derivatives, Heterocycles 67 (2006) 519-522. https:// DOI: 10.3987/COM-05-S(T)52.

[14] R.C. Anand, Vimal, A Mild and Convenient Procedure for the Esterification of Amino Acids, Synth. Comm. 28 (1998) 1963-1965. https://doi.org/10.1080/00397919808007170.

[15] I. Cho, S.H. Kim, J.H. Kim, S. Park, S.Y. Park, Highly efficient and stable deep-blue emitting anthracene-derived molecular glass for versatile types of non-doped OLED applications, J. Mater. Chem. 22 (2012) 123-129. https://doi.org/10.1039/C1JM14482K.

[16] L. Marin, A. van der Lee, S. Shova, A. Arvinte, M. Barboiu, Molecular amorphous glasses toward large azomethine crystals with aggregation-induced emission, New J. Chem. 39 (2015) 6404-6420. https://doi.org/10.1039/C5NJ01052G

[17] E. Cazares-Cortes, B.C. Baker, K. Nishimori, M. Ouchi, F. Tournilhac, Polymethacrylic Acid Shows Thermoresponsivity in an Organic Solvent, Macromolecules 52 (2019) 5995−6004. https://doi.org/10.1021/acs.macromol.9b00412

[18] J. Dong, Y. Ozaki, K. Nakashima, Infrared, Raman, and Near-Infrared Spectroscopic Evidence for the Coexistence of Various Hydrogen-Bond Forms in Poly(acrylic acid), Macromolecules 30 (1997) 1111−1117. https://doi.org/10.1021/ma960693x

[19] S. Morita, Hydrogen-bonds structure in poly(2-hydroxyethyl methacrylate) studied by temperature-dependent infrared spectroscopy, Front. Chem. 2 (2014) 1-5. https://doi.org/10.3389/fchem.2014.00010.

[20] V. Ayzac, Q. Sallembien, M. Raynal, B. Isare, J. Jestin, L. Bouteille, A Competing Hydrogen Bonding Pattern to Yield a Thermo-Thickening Supramolecular Polymer, Angew. Chem. Int. Ed., 58 (2019) 13849-13853. https://doi.org/10.1002/anie.201908954

[21] L.R. Middleton, S. Szewczyk, J. Azoulay, D. Murtagh, G. Rojas, K.B. Wagener, J. Cordaro, K.I. Windey, Hierarchical Acrylic Acid Aggregate Morphologies Produce Strain-Hardening in Precise Polyethylene-Based Copolymers, Macromolecules 48 (2015) 3713-3724. https://doi.org/10.1021/acs.macromol.5b00797.

[22] E.R. Draper, D.J. Adams, Controlling the Assembly and Properties of Low-Molecular-Weight Hydrogelators, Langmuir 35 (2019) 6506–6521. https://doi.org/10.1021/acs.langmuir.9b00716.

[23] C.A. Lagadec, D.K. Smith, Structure–activity effects in peptide self-assembly and gelation – Dendritic versus linear architectures, Chem. Commun. 48 (2012) 7817-7819. https://doi.org/10.1039/C2CC32921B.

[24] M. Kumar, N.L. Ing, V. Narang, N.K. Wijerathne, A.I. Hochbaum, R.V. Ulijn, Amino-acid-encoded biocatalytic self-assembly enables the formation of transient conducting nanostructures, Nature Chem. 10 (2018) 696–703. https://doi: 10.1038/s41557-018-0047-2.

[25] S. Xu, C. Fang, Y. Wu, W. Wu, Q. Guo, J. Zeng, X. Wang, Y. Liu, S. Cao, Photorefractive hyper-structured molecular glasses constructed by calix[4]resorcinarene core and carbazole-based methine nonlinear optical chromophore, Dyes and Pigments 142 (2017) 8-16. https://doi.org/10.1016/j.dyepig.2017.03.001.

[26] F. Rodríguez-Llansola, D. Hermida-Merino, B. Nieto-Ortega, F.J. Ramírez, J.T. López Navarrete, J. Casado, I.W. Hamley, B. Escuder, W. Hayes, J.F. Miravet, Self-Assembly Studies of a Chiral Bisurea-Based Superhydrogelator, Chem., Eur. J. 18 (2012) 14725-14731. https://doi.org/10.1002/chem.201200707

[27] A.R.A Palmans, E.W. Meijer, Amplification of chirality in dynamic supramolecular aggregates, Angew. Chem., Int. Ed. 46 (2007) 8948-8969. https:// DOI: 10.1002/anie.200701285.

[28] A. Plante, D. Mauran, S.P. Carvalho, J.Y.S.D. Pagé, C. Pellerin, O. Lebel, $T_g$ and Rheological Properties of Triazine-Based Molecular Glasses: Incriminating Evidence Against Hydrogen Bonds, J. Phys. Chem. B 113 (2009) 14884-14891. https://doi.org/10.1021/jp905268a.